Paper:

Preliminary Design of a Three-Finger Underactuated Adaptive End Effector with a Breakaway Clutch Mechanism

Kuat Telegenov*, **Yedige Tlegenov***, **Shahid Hussain****, **and Almas Shintemirov***

*Department of Robotics and Mechatronics, School of Science and Technology, Nazarbayev University
53 Kabanbay Batyr Avenue, Astana, Kazakhstan
**School of Mechanical, Materials and Mechatronic Engineering, University of Wollongong
Wollongong, New South Wales 2522, Australia
E-mail: {ktelegenov, yedige.tlegenov, ashintemirov}@nu.edu.kz, mechatronics636@gmail.com
[Received March 16, 2015; accepted July 28, 2015]

Commercially available robotic grippers are often expensive and not easy to modify for specific purposes of robotics research and education. To extend the choice of robotic end effectors available to researchers, this paper presents the preliminary work on prototype design and analysis of a three-finger underactuated robotic end effector with a breakaway clutch mechanism suitable for research in robot manipulation of objects for industrial and service applications. Kinematic models of the finger and the breakaway clutch mechanisms are analyzed aiming to define selection criteria of design parameters. Grasping performance of the end effector prototype manufactured with a 3D printing technology and off-the-shelf components is evaluated using simulation and experimental analyses. Comparison with widely applied available robotic end effectors shows the potential advantages of the proposed end effector design.

Keywords: underactuated robotic end effector, gear train mechanism, breakaway clutch mechanism, 3D printing, adaptive grasping

1. Introduction

Development of robotic end effectors that are employed for grasping of a variety of objects is an active research area. Various robotic end effectors were developed for wide range of applications where reproducing the human hand functionality is desired [1, 2, a]. In most of industrial and service applications manipulation of objects with anthropomorphic robotic hands is not required and two- or three-finger robot end effectors are sufficient for grasping [3]. Examples of such end-effector designs are a microgripper with piezo-actuator for handling very small objects with complex or flexible shapes [4], an intelligent robotic gripper for accurate electronic connector mating [5], a combined gripper with a cutting tool [6] for sweet pepper harvesting, a three-finger pneumatically actuated gripper [7], and an adaptive three-finger robot gripper [b] for use in unstructured industrial applications. A lot of end effector designs utilize individual actuation of each joint of the fingers with small high precision DC servomotors [8, c]. This ensures a high number of controllable degrees of freedom (DOF) suitable for grasping of complex shape objects. However, the presence of multiple actuators in each finger mechanism results in high cost and control complexity of the end effector.

A number of designs utilize pulley/tendon actuation mechanisms that are used for industrial and service robotic systems [9, 10]. These mechanisms have advantages in terms of cost due to less number of actuators, have high degree of adaptability and are suitable for different applications. However, these designs have limitations in load carrying capacity and wear resistance. Tendon excursion must be taken into account during the design process. As an alternative there are many studies reported in literature on different designs of underactuated artificial fingers based on mechanical linkage systems [b, d, e]. Above mentioned end-effectors with mechanical linkage system are complex in their manufacturing and have high number of miniature parts. Thus, there is a need for an end effector, providing configurability for different range of gripping operations with high degree of wear and shock resistance, relatively high payload, simple control systems, and simple mechanical structure [11].

Applications of adaptive mechanical system concepts to design of robotic devices were recently studied in [12]. The presented new design paradigms motivated the authors for this work. The use of mechanical linkage mechanisms in finger design was one of the design criteria to provide relatively high payload carrying capacity comparing to tendon driven systems. Another important design criteria was to use additive manufacturing and simple units for end effector mechanical structure allowing further modification of the proposed design according to specific purposes. Additive manufacturing, or 3D printing, is rapidly maturing with unlimited application potential. Integration of the 3D printing technology in product development process can give the possibility to built products with lighter weight and lower cost but still retain adequate stability and performance [13].

Robotics research and education have gained significant attention in recent years due to increased development and commercial deployment of industrial and service robots. A majority of researchers working on robot grasping and object manipulation utilize commercially available robot-manipulators equipped with various end effectors for experimental studies. Currently available commercial robotic end effectors that are employed for grasping of a variety of objects are expensive and not in mass distribution for research and educational purposes. In general, many of the commercially available hands do not accommodate extensive customisation of the design features for attachment to different robotic arm platforms or integration of additional sensors for research purposes [14]. To address such problems the 3D printing rapid prototyping technology is being actively applied for manufacturing of low-cost robotic hands [15–17].

To extend the choice of robotic end effectors available to researchers, in this paper the authors present a preliminary design and analysis of an underactuated adaptive robotic three-finger end effector. An important characteristic of the presented end effector is provision of the underactuation within the end effector palm and fingers that provides full enveloping of an object without detailed prior knowledge of its shape. Underactuation between fingers is achieved by using a breakaway clutch mechanism, which has novel application to grippers and robotic end effectors. The gripper can be used for various robotics research and educational projects on manipulation of objects in industrial and service applications [18, 19].

The organization of the paper is as follows. In Section 2, the design and analysis of a 2-DOFs underactuated finger and a breakaway clutch mechanisms are outlined in detail. Section 3 presents a design and parameters of the three-finger end-effector. Results of simulation and experimental evaluation of grasping performance of the robotic end effector prototype are presented and discussed in Section 4, which are followed by conclusion and future work.

2. Design of the Underactuated Finger and Breakaway Clutch Mechanism

2.1. Underactuated Finger Mechanism

There has been a long aspiration to reduce the number of actuators and control electronics in robotic end effector designs, that would in turn, lead to reducing of size and mass and cost reduction of the simplified robotic devices. This can be achieved by coupling the motion of numerous joints, resulting to the end effector designs with fewer actuators than DOF. Such robotic end effectors or hands, termed “underactuated,” have shown significant advantages in grasping applications due to the passive flexibility and adaptability between degrees of freedom.

Underactuated fingers with less number of actuators than totals DOFs are widely utilized in design of various robotic hands for industrial [20] and service robotics [21]. This is largely attributed to the relatively simple design of such mechanisms comparing with fully actuated dexterous artificial fingers. At the same time, an underactuated finger mechanism is normally required to provide close wrapping of different shape objects due to its adaptive grasping capability with fewer actuators [22].

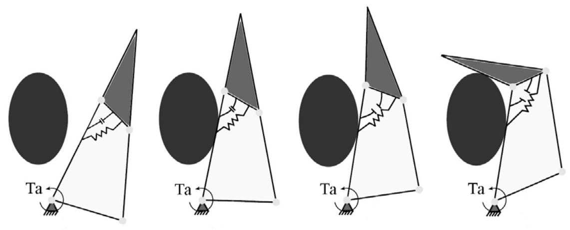

Fig. 1. Closing sequence of a 2-DOF underactuated finger.

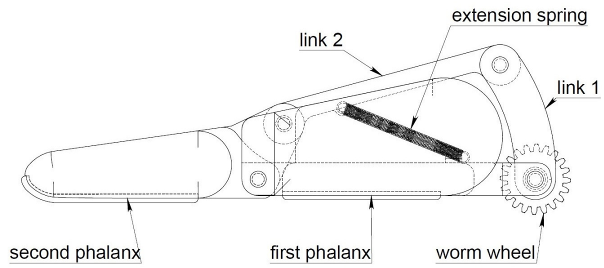

Fig. 2. 2D model underactuated finger.

In this work, the underactuated gripper finger design presented in [23, 24] is adopted. The design utilizes a simple mechanical linkage system which is the one of the main design objectives for the proposed gripper. Consider a 2-DOF and one degree-of-actuation finger mechanism shown in **Fig. 1**. A passive element, i.e., a spring, between the first and second phalanges is used for providing actuation of the second DOF of the finger [23]. The closing sequence of the underactuated finger is described as follows. Firstly, the finger moves as a rigid body from its initial position since no external force is acting on it. When the first phalanx of the finger is in contact with an object, the second phalanx starts movement around a pivot point to complete a full wrapping. Same method can be applied to n-phalanx finger [24]. However, accurate finger mechanism analysis is required to calculate parameters for the passive elements.

Utilizing the same principle, an underactuated finger mechanism has been designed using SolidWorks CAD software and is presented in **Fig. 2**. The finger consists of two phalanges, two links, an extension spring and a worm wheel. Note that the worm wheel and link 1 are rigidly connected. The worm wheel transmits rotary motion to link 1 around its pivot point; subsequently link 1 transfers the motion to link 2. The extension spring, shown in **Fig. 2**, allows the finger to behave as a single rigid body during rotary motion around the fixed pivot. When the first phalanx touches an object, the force produced by an actuator extends the spring which starts transferring motion to the second phalanx only. Finally, the contact of both the phalanges with an object concludes the finger closing sequence.

In overall, the underactuated mechanical linkage sys-

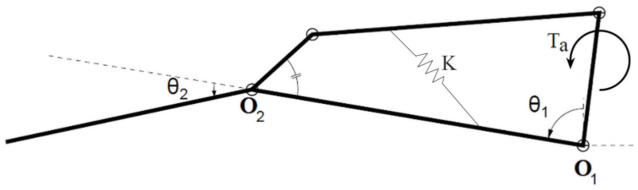

Fig. 3. Schematic model of the 2-DOF underactuated finger.

tem may provide relatively higher load carrying capacity comparing to similar tendon driven mechanisms and requires minimum number of actuators in the gripper. This jointly with utilization of off-the-shelf components and a 3D printing technology ensures lower cost, simple control effort and less weight of the gripper prototype.

Grasping characteristics of the gripper can be modified by setting various geometries of two actuation links of the fingers. For instance, changing the length of two actuation links of the finger can result in various dynamic outputs of the first and second phalanges.

Selection of an appropriate spring stiffness coefficient K_1 that defines actuation of the finger's second phalange is based on the kinematic analysis of the underactuated finger mechanism. The schematic model of the finger is presented in **Fig. 3**. The quasi-static equilibrium modelling of the finger is defined as follows. By equating the input and the output virtual powers [3], the following expression is derived

$$t^T \omega_a = f^T v, \quad (1)$$

where t is the input torque vector, ω_a is the velocity vector, f is the vector of contact wrenches, and v is the vector containing the twist of the contact points [25], defined as

$$t = \begin{bmatrix} T_a \\ T_2 = -K_1 \triangle\theta_2 \end{bmatrix}; \quad \omega_a = \begin{bmatrix} \dot{\theta}_1 \\ \dot{\theta}_2 \end{bmatrix}; \quad (2)$$

$$f = \begin{bmatrix} \zeta_1 \circ \\ \zeta_2 \circ \end{bmatrix}; \quad v = \begin{bmatrix} \xi_1 \\ \xi_2 \end{bmatrix}. \quad (3)$$

Here, T_a denotes the actuation wrench, K is the spring stiffness, $\dot{\theta}_i$ is the first derivative of phalange $i = 1,2$ joint angles. Row vectors $\zeta_i \circ = \begin{bmatrix} m_z & f_i^x & f_i^y \end{bmatrix}$ for $i = 1,2$, are obtained from the corresponding three-dimensional wrench vectors $\zeta_i = \begin{bmatrix} f_i^x & f_i^y & m_z \end{bmatrix}$ by writing the moment m_z of the force axis about the platform center before the force unit vector $f_i = \begin{bmatrix} f_i^x & f_i^y \end{bmatrix}$ [26]. $\xi_i = \begin{bmatrix} \omega_z & \vartheta_i^x & \vartheta_i^y \end{bmatrix}$ is the three-dimensional vector for planar twist.

Substitution of Eqs. (2) and (3) into Eq. (1) yields

$$\begin{bmatrix} T_a & -K_1 \triangle\theta_2 \end{bmatrix} \cdot \begin{bmatrix} \dot{\theta}_1 \\ \dot{\theta}_2 \end{bmatrix} = \begin{bmatrix} \zeta_1 \circ & \zeta_2 \circ \end{bmatrix} \cdot \begin{bmatrix} \xi_1 \\ \xi_2 \end{bmatrix}, \quad (4)$$

from where by equating two matrices from each side the following equation is obtained:

$$T_a \dot{\theta}_{a_1} - K \triangle\theta_2 \cdot \dot{\theta}_2 = \zeta_1 \circ \cdot \xi_1 + \zeta_2 \circ \cdot \xi_2. \quad (5)$$

Thus, the stiffness of the spring can be expressed as

$$K_1 = \frac{T_a \dot{\theta}_1 - \zeta_1 \cdot \circ \xi_1 - \zeta_2 \circ \cdot \xi_2}{\triangle\theta_2 \cdot \dot{\theta}_2} \quad (6)$$

and is used to select appropriate spring for selected finger configuration defined mainly by the actuator characteristics T_a and desired fingertip rotational displacement $\triangle\theta_2$ and its derivative $\dot{\theta}_2$.

Note that the stiffness of the spring K_1 found in Eq. (6) is used in further analysis of the robotic end effector mechanism design.

2.2. Breakaway Clutch Mechanism

With the purpose to achieve adaptive passive grasping of an object the robotic end effector should provide independent actuation of its fingers from each other. Taking into account the requirement to reduce the number of the actuators, the end effector design utilizes the underactuation principle in finger actuation. In this work the authors propose to use a breakaway clutch mechanism with a single actuator, which can provide high underactuation between three fingers of the robotic end effector.

As all three fingers are driven by a single actuator, the actuator drives the fingers through a series of gears. To achieve full wrapping of an object with three fingers by a single actuator, the underactuation principle is used between individual fingers for providing maximum grasp contact. If one finger is blocked by contact of an object, other fingers still continue to move to complete their closing sequence until they contact the grasping object.

In general, the underactuation principle between fingers can be achieved using various differential mechanisms such as gear differentials, linkage seesaw differentials, and pulley differentials [27, 28]. However, application of a gear differential mechanism results to relatively larger space requirements whereas linkage seesaw and pulley differential systems have payload capacity limitations [29].

Previously, a novel breakaway clutch mechanism for accomplishing an enveloping grasping for a three fingered end effector was presented in [30]. However, the proposed mechanism is relatively complex and hard to prototype using 3D printing technology due to low resolution of printing and low elastic modulus of printing materials.

To achieve compatibility with 3D printing technology, the robotic end effector design should utilize simple structural units and have minimal number of miniature parts [15, 16, 28]. Hence, a novel breakaway clutch mechanism for the three fingered robotic end effector is designed and presented in this paper.

The architecture of the breakaway clutch mechanism for a single finger consists of two helical gears, a worm, a worm wheel and a compression spring, and is shown in **Fig. 4**. The driver helical gear rotates the driven helical gear, which in its turn, drives the worm on the same shaft. The driven helical gear and the worm are rigidly connected with the shaft along their vertical axis. The worm transmits motion to the worm wheel, which is pivotally connected to the palm and transmits rotational motion to the finger. The 3D model of the clutch mechanism and its allocation in the palm are presented in **Fig. 5(a)**.

The main reason for utilizing helical gears is that when two helical gear are engaged in motion axial thrust load is

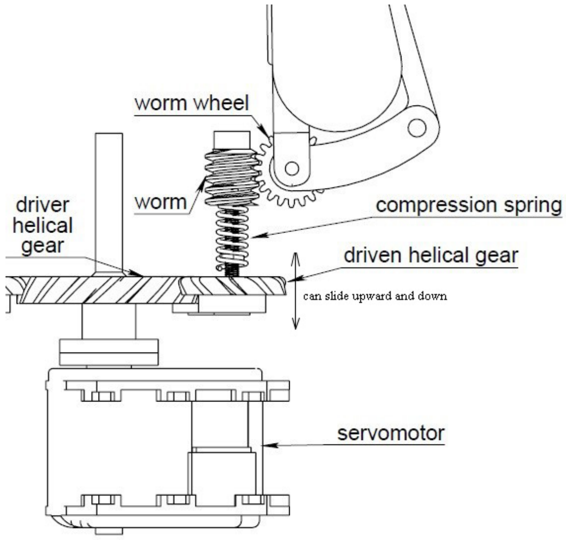

Fig. 4. 2D model of breakaway clutch mechanism.

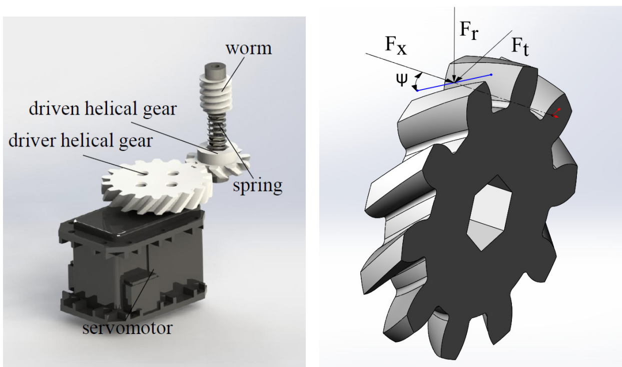

(a) (b)

Fig. 5. (a) 3D CAD model of the breakaway clutch mechanism; (b) a perspective view of the driven helical gear geometry and forces.

produced as a natural result of the inclined arrangement of gear teeth. The driven helical gear is able to slide along its vertical axis while rotating. However, the sliding movement is restricted by the compression spring located between the driven helical gear and the worm on the same shaft. When the compression spring restricts the motion of the driven helical gear, the gear is fully engaged with the driver helical gear. When the finger is in contact with an object the worm movement is fixed, however actuator still continues to move resulting axial thrust force to push the driven helical gear against the spring along its axis. This disengages two helical gears, so the driver helical gear won't transfer any torque to move the finger. Any sliding mechanism can be used for facilitating vertical smooth motion of the driven helical gear.

Analyzing forces acting on a helical gear, shown in **Fig. 5(b)**, it can be seen that axial thrust force F_x acts in the tangential plane parallel to the axis of the shaft carrying the helical gear.

The axial force, F_x tends to push the mating gear along the shaft and is computed as follows:

$$F_x = F_t \tan\psi, \quad \ldots\ldots\ldots\ldots \quad (7)$$

where F_t is the tangential or transmitted force and ψ is a helix angle.

The force $F_t = 2T/D$ is tangential to the pitch surface of the gear and is perpendicular to axis of the shaft carrying the gear. T and D are transmitted torque and pitch diameter of the gear respectively. This is the force that actually drives the gear. The angle ψ defines the angle that teeth are inclined with the axis.

Substituting F_t in Eq. (7) yields

$$F_x = \frac{2T}{D}\tan\psi. \quad \ldots\ldots\ldots\ldots \quad (8)$$

Axial thrust load must be larger than the force exerted by the compression spring to start helical gear sliding upward along its axis.

By Hooke's law the spring force

$$F_s = K_2 x, \quad \ldots\ldots\ldots\ldots \quad (9)$$

where K_2 and x is the stiffness and displacement of the compression spring of the breakaway clutch mechanism respectively.

By equating Eq. (8) to Eq. (9) the equilibrium equation for the breakaway clutch mechanism in vertical direction is obtained. Hence, the stiffness of the compression spring is defined as

$$K_2 = \frac{2T}{Dx}\tan\psi. \quad \ldots\ldots\ldots\ldots \quad (10)$$

The stiffness of the compression spring is the same for the clutches of three fingers in the proposed design.

3. Design of a Three-Finger Robotic End Effector

Three finger robotic end effector includes three underactuated fingers each having two degrees of freedom, a frame housing a palm, the breakaway clutch mechanism and an actuator. The finger arrangement on the palm allows the gear trains of the fingers to be driven from a single actuator. Two fingers are placed opposite to each other whereas the third finger is adjusted to one of them by certain angle. This design solution allows the end effector to perform planar grasping of tiny objects. Each finger is actuated through the breakaway clutch mechanism, discussed in Section 3, containing a worm wheel that enables self-locking property of each finger in their closing and opening sequence when the actuator is powered off [11].

The CAD model of the proposed robotic end effector and its 3D printed assembled prototype are presented in **Fig. 6**. The prototype main structures are manufactured using the UP Plus 3D printer [f] with acrylonitrile butadiene styrene (ABS) plastic, whereas soft rubber printing material are used for producing fingertip, phalange and palm covers. ABS is a strong, durable production-grade thermoplastic used across many industries, and it is an

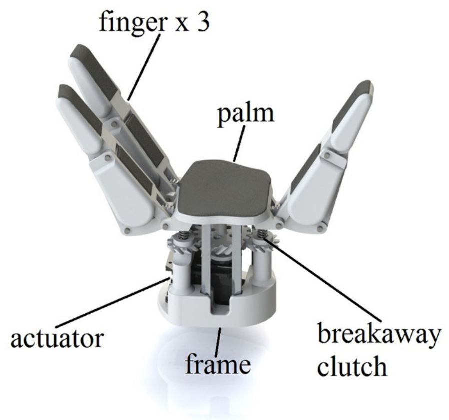

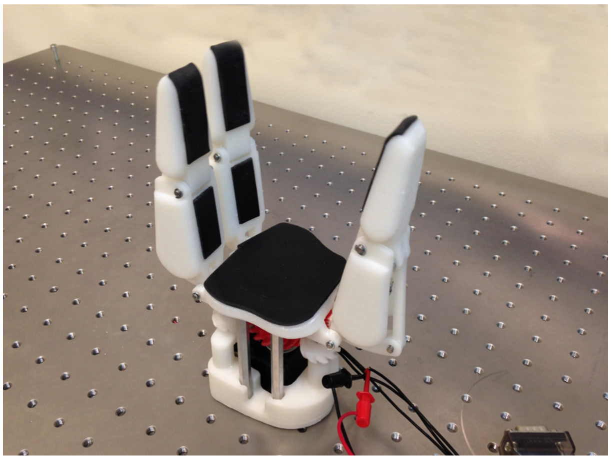

Fig. 6. 3D CAD model and prototype of a three-finger robotic end effector.

ideal material for conceptual prototyping [g]. An additional off-the-shelf component, a Dynamixel MX-28 servomotor [h], is used as an actuator for the end effector prototype that eliminates necessity for complex electronic circuits and encoders implementing motor position control. Control of the servomotor can be performed directly from MATLAB or C/C++ programming environments as well as using the Robot Operating System (ROS) [i], that provide easy and straightforward integration of the gripper with other robotic research and educational setups. The output torque of the servomotor is 2.5 Nm at 12 V power supply voltage.

Combining the finger and the breakaway clutch mechanisms into a single system requires selecting appropriate parameters for the springs in the clutch and finger mechanisms. For proper grasping of an object each finger mechanism should perform the closing sequence to a full possible extent independently of each other. This is achieved in the case when stiffness of the spring in the clutch is larger than stiffness of the spring in the finger as shown below

$$K_1 \leq K_2. \qquad (11)$$

In the proposed gripper design actuation wrench T_a is applied to the pivot point of the finger, transferring rotational motion. Having one actuator and three fingers the actuation wrench of each finger can be calculated knowing transmitted torque T as follows:

$$T_a = \frac{\zeta_1 \circ \xi_1 - \zeta_2 \circ \xi_2}{\dot{\theta}_1} + \frac{2T\Delta\theta_2\dot{\theta}_2}{Dx\dot{\theta}_1}\tan\psi. \qquad (12)$$

Thus, using Eqs. (11) and (12) the end effector design parameters can be determined providing the desired actuation wrench and the torque applied from the output shaft of the actuator are known.

In the robotic end effector prototype the output shaft of the Dynamixel actuator is directly connected to an eighteen teeth helical gear with 1.5 inches pitch diameter, which drives three smaller ten teeth helical gears, with 0.833 inches pitch diameters, one for each finger mechanism. The three helical gears rotate together with three worms having one thread and 0.8 module parameters. Finally, the three worms transfer rotational motion to three twenty teeth worm wheels with 0.62 inches pitch diameters, which are connected to the finger mechanism.

4. Results and Discussions

4.1. Simulation Results

Simulation analysis of the end effector grasping performance is done using the ADAMS mechanical system modeling software. The prototype geometrical parameters are set in the program, according to the chosen finger design dimensions, whereas mass properties are defined by setting the model material density as ABS plastic used for the prototype 3D printing. The two-phalanx finger linkage system is pivotally connected to a fixed point on the origin of a working grid; other joints can revolute unless otherwise stated.

For motion simulation shown the finger actuation torque is applied to link 1 around pivot point O_1 as shown in **Fig. 3**. To provide actuation to the second DOF for the finger an extension spring is placed between links 1 and 2. Actuation torque is calculated according to characteristics of the chosen actuator. All gear ratios are calculated and included in simulation. **Fig. 7** illustrates the simulation results of the finger grasping sequence that correlate well with the theoretical grasping sequence of an underactuated finger linkage mechanism described in Section 2. The ball shape in the figure represents a grasping object and is fixed to the workspace. The gravity is taken into account and applied in the vertical direction downwards.

4.2. Experimental Results

The main grasping patterns of the robotic gripper can be summarized to three main configurations: cylindrical, spherical and planar [22], as illustrated in **Fig. 8**. All three fingers of the robotic gripper are pivoted to the palm in a way that allows executing the grasping configurations without changing orientations of the finger bases. This feature greatly simplifies the end effector design.

Figure 9 illustrates the performance of the proposed robotic end effector while grasping a number of objects

Fig. 7. Simulation carried out on ADAMS showing grasping sequence.

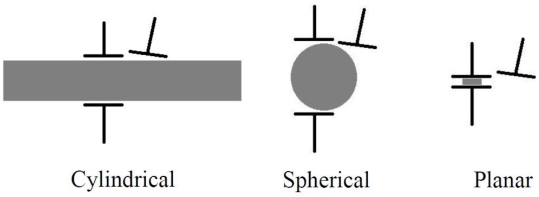

Fig. 8. Grasping configurations of the end effector.

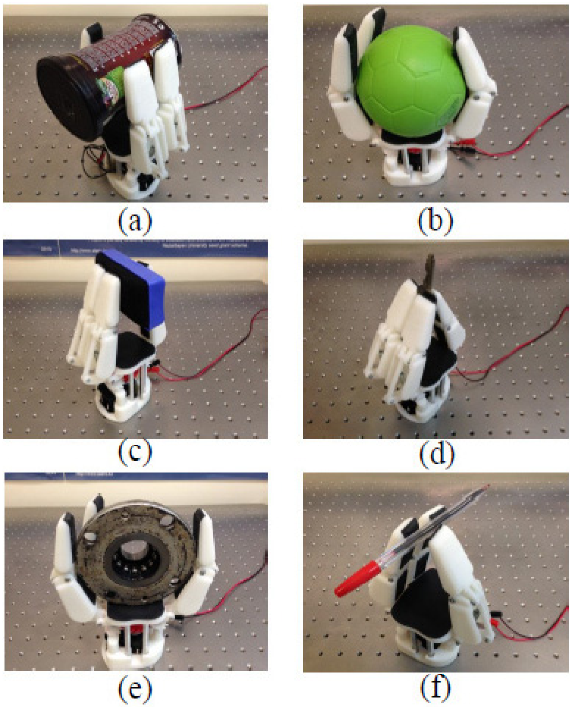

Fig. 9. Grasping of different objects by the robotic end effector prototype: (a) cylindrical grasp. (b) Spherical grasp. (c) Planar grasp. (d) Fingertip grasp. (e) High payload, large shape grasp. (f) Low payload, small shape grasp.

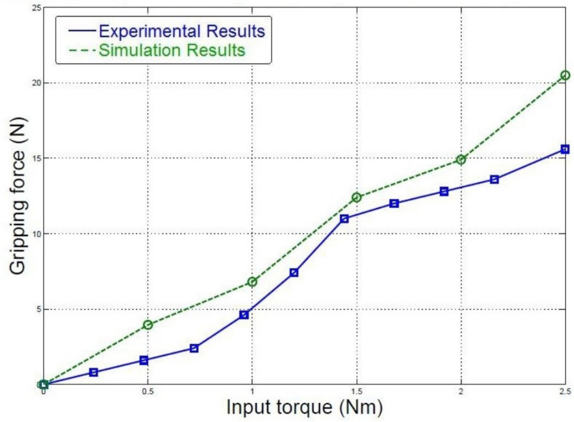

Fig. 10. The relationship of the grasping force versus input torque.

with different shapes. It can be seen that the end effector fingers are able to adapt to the shapes of the grasped objects. For instance, the cylindrical grasping pattern is achieved by holding an object with two fingers situated opposite to each other, whereas the third finger ensures the grasp stability. This prevents unstable grasps and allows gripping cylindrical objects without prior knowledge of their center of mass. During spherical grasping fingers adapt to the shape of the object and fully envelope it. Planar grasping is performed at tip phalanxes using all three fingers, while fingertip grasp uses only two fingers for picking up small objects. The video of the gripper performance is available at www.alaris.kz.

The relationship of the gripping force vs. input torque of the designed robotic end effector is theoretically simulated and experimentally obtained using a force gauge measuring applied gripping force at fingertips as shown in **Fig. 10**. It can be clearly seen that there is a slight difference of the gripping force between simulated and experimental results which might be attributed to energy loss between moving parts of the end effector prototype. The maximum gripping force of the robotic end effector prototype was experimentally estimated as 15 N. However, due to non-backdrivability of the end effector actuating mechanism, the fingers may resist much larger forces that they actually exert [11].

A comparison of the proposed robotic end effector with widely applied three-finger robotic end effectors is presented in **Table 1**. The end effectors have been developed for different (e.g., industrial: Barrett Hand, Robotiq, Schunk SDH Hand, or service: Kinova JACO, i-HY Hand) applications. The number of utilized actuators is used as one of the comparative parameters due to its effect on the overall cost and power requirements for a robotic end effector [31]. As clear from **Table 1** the designed robotic end effector in this paper rovides comparable gripping force characteristics and available types of

Table 1. Comparison of three-finger robotic end effectors.

Hand	Type of grasping	No. of actuators	Gripping force [N]
Barrett Hand	C S	4	15
Robotiq	C S P	2	15–60
Schunk SDH Hand	C S P	7	–
Kinova JACO	C S P	3	–
SDM Hand	C S	1	10
Presented End effector	C S P	1	10–15

grasping, i.e., cylindrical (C), spherical (S) and planar (P) grasps (**Fig. 8**), with respect to the commercially available robotic devices. In addition, the use of minimum number of actuators and the 3D printing technology makes the proposed design potentially preferable in terms of the cost to payload ratio.

5. Conclusions

This paper presents authors' preliminary work on the design of an underactuated robotic end effector with a breakaway clutch mechanism. A novel application of a breakaway clutch mechanism using helical gears is presented. This mechanism provides independent movement of the fingers actuated by a single actuator. The end effector design model and its experimental prototype are introduced and discussed in detail. It is shown that the the presented robotic end effector with one actuator meets the design objectives in terms of:

- simple mechanical structure of the end effector due to usage of a four-bar linkage system;
- a low cost due to usage of a single actuator, 3D printing prototyping technology and off-the-shelf components;
- relatively high payload comparable with currently available robotic end effectors.

In overall, the proposed end effector design can be potentially preferable in terms of cost to payload ratio.

Future work includes design and implementation of proposed end effector prototype with embedded sensing elements such as tactile sensors for force feedback capabilities and depth camera for object recognition to perform autonomous grasping performance. The end effector prototype will be mounted on an industrial manipulator for evaluating grasping performance in real-life scenarios.

References:

[1] S. Jacobsen, E. Iversen, D. Knutti, R. Johnson, and K. Biggers, "Design of the Utah/M.I.T. Dextrous Hand," Proc. of the 1986 IEEE Int. Conf. on Robotics and Automation, pp. 1520-1532, 1986.

[2] M. Baril, T. Laliberte, C. Gosselin, and F. Routhier, "On the Design of a Mechanically Programmable Underactuated Anthropomorphic Prosthetic Gripper," ASME J. of Mechanical Design, Vol.135, No.12, p. 121008, 2013.

[3] T. Laliberte, L. Birglen, and C. Gosselin, "Underactuation in robotic grasping hands, Machine Intelligence & Robotic Control," Vol.4, No.3, pp. 1-11, 2002.

[4] Y. Ando, "Microgripper," J. of Robotics and Mechatronics, Vol.2, No.3, pp. 214-216, 1990.

[5] F. Chen, K. Sekiyama, B. Sun, P. Di, J. Huang, H. Sasaki, and T. Fukuda, "Design and Application of an Intelligent Robotic Gripper for Accurate and Tolerant Electronic Connector Mating," J. of Robotics and Mechatronics, Vol.24, No.3, pp. 441-451, 2012.

[6] S. Bachche and K. Oka, "Design, Modeling and Performance Testing of End-Effector for Sweet Pepper Harvesting Robot Hand," J. of Robotics and Mechatronics, Vol.25, No.4, pp. 705-717, 2013.

[7] G. Figliolini and M. Sorli, "Open-Loop Force Control of a Three-Finger Gripper Through PWM Modulated Pneumatic Digital Valves," J. of Robotics and Mechatronics, Vol.12, No.4, pp. 480-493, 2000.

[8] A. Namiki, Y. Imai, M. Kaneko, and M. Ishikawa, "Development of a High-Speed Multifingered Hand System," Proc. of the 2003 IEEE/RSJ Int. Conf. on Intelligent Robots and Systems, pp. 2666-2671, 2004.

[9] W. Townsend, "The Barret Hand grasper - programmably flexible part handling and assembly," Industrial Robot, Vol.27, pp. 181-188, 2000.

[10] L. U. Odhner et al., "A compliant, underactuated hand for robust manipulation," Int. J. of Robotics Research, Vol.33, No.5, pp. 736-752, 2014.

[11] S. J. Bartholet, "Reconfigurable end effector," U.S. Patent No:5108140, 1992.

[12] C. Gosselin, "Adaptive Robotic Mechanical Systems: A Design Paradigm," ASME J. of Mechanical Design, Vol.128, No.1, pp. 192-198, 2005.

[13] C. Beyer, "Strategic implications of current trends in additive manufacturing," ASME J. of Manufacturing Science and Engineering, Vol.136, No.6, p. 064701, 2014.

[14] R. R. Ma, L. U. Odhner, and A. M. Dollar, "A modular, open-source 3D printed underactuated hand," Proc. of the 2013 IEEE Int. Conf. on Robotics and Automation, pp. 2737-2743, 2013.

[15] Z. Kappassov, Y. Khassanov, A. Saudabayev, A. Shintemirov, and H. A. Varol, "Semi-anthropomorphic 3D printed multigrasp hand for industrial and service robots," Proc. of the 2013 IEEE Int. Conf. on Mechatronics and Automation, pp. 1697-1702, 2013.

[16] Y. Tlegenov, K. Telegenov, and A. Shintemirov, "An open-source 3D printed underactuated robotic gripper," Proc. of the 10th IEEE/ASME Int. Conf. on Mechatronic and Embedded Systems and Applications, pp. 1-6, 2014.

[17] C. Chen, "Mechatronics Design of Multi-Finger Robot Hand," 12th Int. Conf. on Control, Automation and Systems, pp. 1491-1496, 2012.

[18] C. Liu, H. Qiao, J. Su, and P. Zhang, "Vision-based 3-D grasping of 3-D objects with a simple 2-D gripper," IEEE Trans. on Systems, Man, and Cybernetics: Systems, Vol.44, pp. 605-620, 2014.

[19] J. M. Romano, K. Hsiao, G. Niemeyer, S. Chitta, and K. J. Kuchenbecker, "Human-inspired robotic grasp control with tactile sensing," IEEE Trans. on Robotics, Vol.27, pp. 1067-1079, 2011.

[20] T. Laliberte and C. Gosselin, "Actuation system for highly underactuated gripping mechanism," U.S. Patent No:6505870, 2003.

[21] L. J. Caron and C. Deguire, "Mechanical Finger," PCT Patent WO2010/142043 A1, 2010.

[22] T. Laliberte and C. Gosselin, "Underactuation in space robotic hands," Int. Symposium on Artificial Intelligence, Robotics and Automation in Space, pp. 18-21, 2001.

[23] S. Montambault and C. Gosselin, "Analysis of Underactuated Mechanical Grippers," ASME J. of Mechanical Design, Vol.123, No.3, pp. 367-374, 2001.

[24] L. Birglen and C. Gosselin, "Geometric design of three-phalanx underactuated fingers," ASME J. of Mechanical Design, Vol.128, No.2, pp. 356-364, 2005.

[25] L. Birglen and C. Gosselin, "Kinetostatic analysis of underactuated fingers," IEEE Trans. on Robotics and Automation, Vol.20, No.2, pp. 211-221, 2004.

[26] I. A. Bonev, D. Zlatanov, and C. Gosselin, "Singularity Analysis of 3-DOF Planar Parallel Mechanisms via Screw Theory," ASME J. of Mechanical Design, Vol.125, No.3, p. 537-581, 2003.

[27] L. Birglen and C. Gosselin, "Force analysis of connected differential mechanisms: application to grasping," Int. J of Robotics Research, Vol.25, No.10, pp. 1033-1046, 2006.

[28] R. R. Ma, L. U. Odhner, and A. M. Dollar, "A modular, open-source 3D printed underactuated hand," Proc. of the 2013 IEEE Int. Conf. on Robotics and Automation, pp. 2737-2743, 2013.

[29] K. Telegenov, Y. Tlegenov, and A. Shintemirov, "An underactuated adaptive 3D printed robotic gripper," Proc. of the 10th France-Japan/8th Europe-Asia Congress on Mechatronics, pp. 110-115, 2014.

[30] N. T. Ulrich, "Methods and apparatus for mechanically intelligent grasping," U.S. Patent No:4957320, 1990.

[31] S. Hussain, Q. Xie, and P. K. Jamwal, "Control of a Robotic Orthosis for Gait Rehabilitation," Robotics and Autonomous Systems, Vol.61. No.911-919, 2013.

Supporting Online Materials:

[a] Shadow Dexterous Hand Technical Specification, 2013
http://www.shadowrobot.com/wp-content/uploads/
shadow_dexterous_hand_technical_specification_E1_20130101.pdf
[Accessed October 2, 2014]

[b] Robotiq, Three-Finger Adaptive Robot Gripper
http://robotiq.com/media/Robotiq-3-Finger-Adaptive-Robot-Gripper-Specifications.pdf [Accessed October 10, 2014]

[c] Schunk, Servo-Electric 3-Finger Gripping Hand SDH
http://www.schunk.com/schunk_files/attachments/SDH_DE_EN.pdf
[Accessed November 2, 2014]

[d] Delft University of Technology, Delft Hand
http://www.3me.tudelft.nl/en/about-the-faculty/departments/
biomechanical-engineering/research/dbl-delft-biorobotics-lab/
delft-arm-and-hand/ [Accessed October 15, 2014]

[e] Kinova, JACO Research Edition
http://kinovarobotics.com/wp-content/uploads/2013/05/
kinova-jaco-spec-sheet.pdf [Accessed November 5, 2014]

[f] UP Plus 3D Printer, http://www.pp3dp.com/
[Accessed September 20, 2014]

[g] Stratasys ABS Material Properties
http://www.nrri.umn.edu/NLTC/ABS07.pdf
[Accessed February 2, 2014]

[h] Robotis, Dynamixel MX-28, http://support.robotis.com/en/product/dynamixel/mx_series/mx-28.htm [Accessed February 15, 2015]

[i] The Robot Operating System (ROS), http://www.ros.org
[Accessed August 19, 2014]

Name:
Kuat Telegenov

Affiliation:
Department of Robotics and Mechatronics, School of Science and Technology, Nazarbayev University

Address:
53 Kabanbay Batyr Avenue, Astana, Kazakhstan

Brief Biographical History:
2012 Received B.Sc. degree in Mechanical Engineering (Aeronautics) from University Technology of Malaysia
2014 Received M.Sc. degree in Mechanics from Gumilyov Eurasian National University
2015- Instructor, Department of Robotics and Mechatronics, Nazarbayev University

Main Works:
• robotics, mechanical design, underactuated mechanisms

Name:
Yedige Tlegenov

Affiliation:
Department of Robotics and Mechatronics, School of Science and Technology, Nazarbayev University
National University of Singapore

Address:
53 Kabanbay Batyr Avenue, Astana, Kazakhstan

Brief Biographical History:
2011 Received B.Sc. degree in Mechanics from Gumilyov Eurasian National University
2013 Received M.Sc. degree from Anna University
2013- Ph.D. Student, National University of Singapore
2013- Department of Robotics and Mechatronics, Nazarbayev University

Main Works:
• parallel mechanisms, robot vehicles and industrial design

Name:
Shahid Hussain

Affiliation:
School of Mechanical, Materials and Mechatronics Engineering, University of Wollongong

Address:
New South Wales 2522, Australia

Brief Biographical History:
2007 Received B.Sc. in Mechatronics and Control Engineering from University of Engineering and Technology Lahore
2009/2013 Received M.Sc. and Ph.D. in Mechanical Engineering from University of Auckland
2013- Lecturer, School of Mechanical, Materials and Mechatronics Engineering, University of Wollongong

Main Works:
• robot compliant actuation, robot assisted rehabilitation, robust and adaptive control of compliant robotic manipulators

Name:
Almas Shintemirov

Affiliation:
Department of Robotics and Mechatronics, School of Science and Technology, Nazarbayev University

Address:
53 Kabanbay Batyr Avenue, Astana, Kazakhstan

Brief Biographical History:
2001 Received Engineer's degree from Pavlodar State University
2004 Received Candidate's degree in Technical Sciences (Ph.D.) from Pavlodar State University
2009 Received Ph.D. in Electrical Engineering and Electronics from University of Liverpool
2011- Assistant Professor, Department of Robotics and Mechatronics, Nazarbayev University

Main Works:
• robotic/mechatronic system design and computation intelligence

Membership in Academic Societies:
• The Institute of Electrical and Electronics Engineers (IEEE) Robotics and Automation Society